ResearchGate

See discussions, stats, and author profiles for this publication at: https://www.researchgate.net/publication/49805679

Engineered dimer interface mutants of triosephosphate isomerase: The role of inter-subunit interactions in enzyme function and stability

Article *in* Protein Engineering Design and Selection · February 2011

DOI: 10.1093/protein/gzr005 · Source: PubMed

CITATIONS
6

READS
93

4 authors, including:

Mousumi Banerjee
Indian Institute of Science Education and Research, Tirupati
16 PUBLICATIONS **158** CITATIONS

SEE PROFILE

niranjan.v. Joshi
Indian Institute of Science
122 PUBLICATIONS **3,003** CITATIONS

SEE PROFILE

Padmanabhan Balaram
Indian Institute of Science
595 PUBLICATIONS **19,813** CITATIONS

SEE PROFILE

Some of the authors of this publication are also working on these related projects:

Harvard _ post doc at RB Woodward View project

Bioactive peptides View project

All content following this page was uploaded by niranjan.v. Joshi on 02 February 2016.

The user has requested enhancement of the downloaded file.

Protein Engineering, Design & Selection vol. 24 no. 5 pp. 463–472, 2011
Published online February 2, 2011 doi:10.1093/protein/gzr005

Engineered dimer interface mutants of triosephosphate isomerase: the role of inter-subunit interactions in enzyme function and stability

Mousumi Banerjee[1], Hemalatha Balaram[2], N.V.Joshi[3] and P.Balaram[1,4]

[1]Molecular Biophysics Unit, Indian Institute of Science, Bangalore 560012, India, [2]Molecular Biology and Genetics Unit, Jawaharlal Nehru Centre for Advanced Scientific Research, Jakkur, Bangalore 560064, India and [3]Centre for Ecological Sciences, Indian Institute of Science, Bangalore 560012, India

[4]To whom correspondence should be addressed.
E-mail: pb@mbu.iisc.ernet.in

Received December 25, 2010; revised December 25, 2010; accepted January 5, 2011

Edited by Rik K. Wierenga

The role of inter-subunit interactions in maintaining optimal catalytic activity in triosephosphate isomerase (TIM) has been probed, using the *Plasmodium falciparum* enzyme as a model. Examination of subunit interface contacts in the crystal structures suggests that residue 75 (Thr, conserved) and residue 13 (Cys, variable) make the largest number of inter-subunit contacts. The mutants Cys13Asp (C13D) and Cys13Glu (C13E) have been constructed and display significant reduction in catalytic activity when compared with wild-type (WT) enzyme (∼7.4-fold decrease in k_{cat} for the C13D and ∼3.3-fold for the C13E mutants). Analytical gel filtration demonstrates that the C13D mutant dissociates at concentrations <1.25 μM, whereas the WT and the C13E enzymes retain the dimeric structure. The order of stability of the mutants in the presence of chemical denaturants, like urea and guanidium chloride, is WT > Cys13Glu > Cys13Asp. Irreversible thermal precipitation temperatures follow the same order as well. Modeling studies establish that the Cys13Asp mutation is likely to cause a significantly greater structural perturbation than Cys13Glu. Analysis of sequence and structural data for TIMs from diverse sources suggests that residues 13 and 82 form a pair of proximal sites, in which a limited number of residue pairs may be accommodated.

Keywords: dimer stability/inter-subunit interactions/*Plasmodium falciparum*/subunit interface/triosephosphate isomerase

Introduction

Triosephosphate isomerase (TIM) catalyzes the reversible isomerization of dihydroxyacetone phosphate (DHAP) and glyceraldehyde 3-phosphate (GAP), a central step in the glycolytic pathway (Rieder and Rose, 1959; Wierenga *et al*., 2010). This deceptively simple chemical reaction requires the stereospecific abstraction of a proton bonded to a carbon atom followed by re-protonation at the adjacent carbon atom (Putman *et al*., 1972; Webb and Knowles, 1974, 1975). Extensive structural, kinetic and mutagenesis studies have provided a detailed picture of the mechanism leading Jeremy Knowles to call TIM 'an evolutionary perfect enzyme' (Albery and Knowles, 1976a,b; Knowles, 1991). Despite the extensive dissection of the TIM mechanism (Lodi and Knowles, 1991; Cui and Karplus, 2003), protein design experiments to engineer TIM active sites on to other protein scaffolds have proved unsuccessful (Dwyer *et al*., 2004, 2008). TIM functions as a dimeric enzyme in bacteria and eukaryotes, while the archaeal enzyme is a tetramer, as demonstrated by studies on the proteins from *Pyrococcus woesei* and *Methanocaldococcus jannaschii* (Casal *et al*., 1987; Borchert *et al*., 1993; Schliebs *et al*., 1997; Walden *et al*., 2001; Gayathri *et al*., 2007). Several studies have attempted to address the question of whether TIM is an obligate dimer. Attempts to engineer monomeric TIMs have resulted in well-folded (α_8/β_8) barrel structures, whose catalytic activity is reduced by >1000-fold (Borchert *et al*., 1993, 1994). The critical residues at the TIM active site, Lys12, His95 and Glu165, which surround the substrate, are all located on one subunit. The availability of a high-resolution crystal structure of the yeast TIM–DHAP complex [protein data bank (PDB) ID 1NEY] (Jogl *et al*., 2003) provides many insights into the positioning of the substrate with respect to key catalytic residues involved in the proton transfer reaction. The sharp fall in enzymatic activity in engineered monomers suggests that functional active site construction must involve critical interactions at the subunit interface. Figure 1 schematically summarizes the peptide segments that provide a maximum number of inter-subunit contacts (≤4 Å) in *Plasmodium falciparum* TIM (PfTIM) (Singh *et al*., 2001; Maithal *et al*., 2002). Bacterial and eukaryotic TIMs have a polypeptide chain length of 240–270 residues, with PfTIM having a length of 248 residues. The segments comprising the dimer interface lie within the first 100 residues. Four distinct segments that comprise the interacting surface may be identified.

A feature of the malarial parasite enzyme, also present in the enzymes from *Trypanosoma* and *Leishmania*, is the occurrence of a Cys residue at position 13, adjacent to the active site Lys12 residue (Wierenga *et al*., 1987; Ostoa-Saloma *et al*., 1997). (We use here the residue numbering scheme for the *P.falciparum* enzyme. Numbering schemes for PfTIM and yeast TIM are identical for the fragments 1–32 and 58–248. Residues 34–57 of PfTIM correspond to residues 33–56 of yeast TIM.) In the human enzyme methionine (Met) occurs at this position, leading to attempts to develop sulfhydryl modifiers as site-directed inhibitors of the parasite enzymes (Gómez-Puyou *et al*., 1995; Garza-Ramos *et al*., 1996; Joubert *et al*., 2001; Cortés-Figueroa *et al*., 2008). Inspection of Fig. 1 reveals that the largest number of interface contacts

© The Author 2011. Published by Oxford University Press. All rights reserved.
For Permissions, please e-mail: journals.permissions@oup.com

Downloaded from peds.oxfordjournals.org at Indian Institute of Science on May 26, 2011

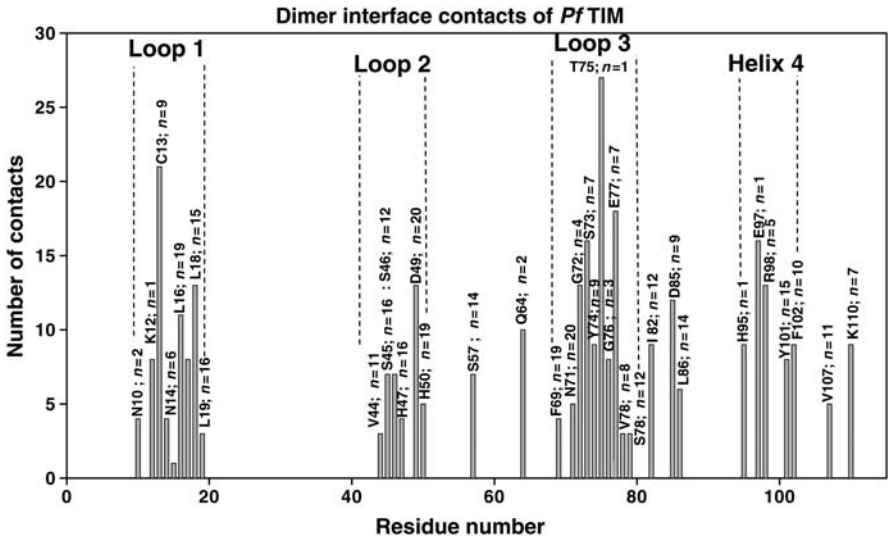

Fig. 1. A stick plot summarizing the residue contacts across the subunit interface (dimer interface) in *P.falciparum* TIM structure (PDB ID 1O5X). A distance cutoff $\leq$4 Å was used to identify the residues. Residues 1–110 are shown here. Residues toward the C-terminal half do not contribute to the dimer interface. The numbers on each bar represent the number of different amino acids at that particular position, in natural sequences. A curated dataset of 470 non-archaeal (bacterial and eukaryotic) TIM natural sequences were analyzed.

is made by the fully conserved Thr75 residue, which is important in maintaining active site architecture, and Cys13, which is a variable residue in sequences from diverse organisms. A double mutant, constructed by Wierenga and coworkers, derived by replacement of T75 and G76 by R75 and E76 resulted in a monomeric protein in solution (known as RE mutant), with reduced catalytic activity compared with the wild type (WT) (k_{cat} for WT $= 3.7 \times 10^5$ min^{-1} and k_{cat} for RE mutant $= 1.3 \times 10^2$ min^{-1}) (Schliebs *et al.*, 1997). Figure 2 shows a view of the inter-subunit interaction involving the Cys13 residue and the loop 3 segment (residues 71–79) in PfTIM. It is evident that multiple hydrogen bonding interactions involving the Cys13 backbone and the thiol S–H group may contribute to the stability of the dimer. Multiple sequence alignment of a curated dataset of 470 non-archeal TIM sequences revealed the distribution of residues at position 13, summarized in Fig. 2B. In the overwhelming majority of sequences, Met occurs at this position, while eight other residues are also seen. The absence of charged and aromatic amino acids is striking. We therefore chose to examine the effects of introducing the negatively charged residues Asp (D) and Glu (E), in order to probe effects on dimer stability and enzymatic activity.

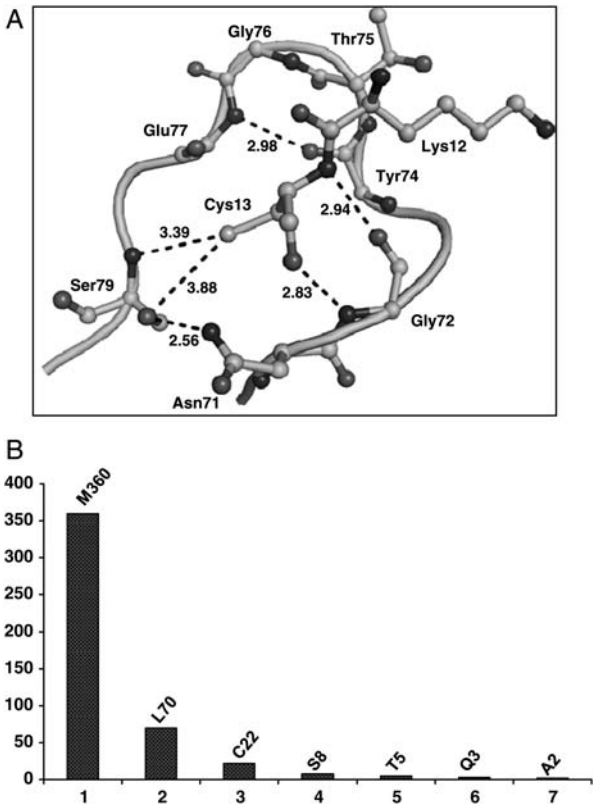

Fig. 2. (**A**) The environment of Cys13 residue in one subunit of PfTIM (PDB ID 1O5X). Residues from the adjacent subunit are also shown here. The critical hydrogen bonds formed by the backbone and the side chain atoms of Cys13 are shown as dotted lines. The image was generated using PyMol (DeLano, 2002). (**B**) The frequency distribution of different amino acids at position 13 in natural sequences. A curated dataset of 470 unique natural TIM sequences (bacterial and eukaryotic) was analyzed.

Materials and methods

All media components were purchased from HiMedia Laboratories (Mumbai, India). Substrates used for enzyme assays, buffer components, protein molecular weight markers, urea and guanidine hydrochloride were purchased from Sigma Chemical Company (St Louis, MO, USA). All reagents were of analytical grade. Akta Basic HPLC, Superdex 200 and Q-sepharose columns were from GE Healthcare (India). All assays were done using a JASCO-710 (Tokyo, Japan) spectrophotometer and a JASCO-715 spectropolarimeter (Tokyo, Japan) fitted with a water-circulated cell holder. The temperature was maintained using a Julabo (JULABO Labortechnik GmbH, Seelbach, Germany) circulating water bath.

Site-directed mutagenesis

Wild-type PfTIM gene was cloned in pTrc99A vector and expressed in AA200 *Escherichia coli* cells (TIM null mutants) (Ranie *et al.*, 1993). The Asp (D) and Glu (E)

Downloaded from peds.oxfordjournals.org at Indian Institute of Science on May 26, 2011

mutants at position 13 were generated using the 'megaprimer' polymerase chain reaction (PCR) method (Sarkar and Sommer, 1990). The oligonucleotides used in this study are C13D: 5′CCACATGGCTAGAAAATATTTTGTCGCAGCAAACTG GAAAGAAATGGAACT3′ and C13E: 5′CACCATGGCTAG AAAATATTTTGTCGCAGCAAACTGGAAAGAAAATGG A3′. Briefly, the mutants were generated using two rounds of PCR. In the first round, the megaprimer was generated along with the mutation, and in the second round the full-length gene was amplified using the C-terminal WT primer of TIM gene. Each 50 μl PCR mixture contained 200 ng of each primer, 20 ng of the template, 200 μM of each dNTP and 5 U of *Taq* DNA polymerase. The PCR cycle used was denaturation at 94°C for 4 min to give a hot start, then 93°C for 25 s, annealing at 48°C for 50 s and extension at 73°C for 35 s. The product obtained, after 30 cycles of PCR, was purified by elution from agarose gels and used as a megaprimer in a second round of PCR. The other primers used in the PCR amplification are TIM forward primer: 5′-CAGAAT TCCATGGCTAGAAAATATTTTGTCGC-3′ and TIM reverse primer: 5′-ACGGATCCTTACATAGCACTTTTTATTAT ATC-3′.

The second PCR condition was 94°C for 4 min to give a hot start, then 93°C for 30 s, annealing at 52°C for 50 s and extension at 73°C for 1 min. After 30 cycles a final extension of 10 min at 72°C was allowed. The full-length amplified product containing the desired mutation was purified using a gene cleaning kit (QIAGEN), digested with enzymes NcoI and BamHI, and ligated to the vector pTrc99A, digested with the same enzymes. Recombinants were selected after transformation into the *E.coli* strain DH5α on the basis of supercoiled plasmid mobility (Sambrook and Russell, 2001). The presence of insert was confirmed by restriction digestion at sites that were incorporated in the mutagenic primers. The clones were sequenced (Microsynth, Switzerland) to confirm the mutation.

Protein expression and purification

Expression of the TIM gene was performed using the pTrc99A system. *E.coli* AA200 (a null mutant of inherent TIM gene) cells carrying the pTrc99A-recombinant vector were grown at 37°C in Terrific broth containing 100 μg ml^{-1} ampicillin. Cells were induced using 300 μM isopropyl-β-D-thiogalactopyranoside at 0.6–0.8 OD600 nm and were harvested by centrifugation (15 min, 6000 rpm, 4°C). Cells were resuspended in lysis buffer, containing 20 mM Tris–HCl (pH 8.0), 1 mM EDTA, 0.01 mM phenylmethanesulfonyl fluoride, 2 mM dithiothreitol (DTT) and 10% glycerol and disrupted using sonication. After centrifugation (45 min, 12 000 rpm, 4°C), the supernatant was fractionated using ammonium sulfate. The protein fraction containing TIM was precipitated between 60 and 80% ammonium sulfate saturation. This precipitate was collected by centrifugation (30 min, 12 000 rpm, 4°C) and resuspended in buffer-A [20 mM Tris–HCl (pH 8.0), 2 mM DTT and 10% glycerol]. Monitoring of each step was performed by sodiumdodecyl sulfate-polyacrylamide gel electrophoresis (SDS-PAGE) analysis (12% polyacrylamide). Nucleic acid was removed using polyethyleneimine precipitation and the succeeding purification steps were conducted at 4°C. The protein was dialyzed extensively against buffer-A at 4°C overnight and purified using an anion exchange (Q-sepharose, HR 60) column and eluted with a linear gradient of 0–1 M NaCl. The fractions containing the protein were pooled and precipitated by addition of ammonium sulfate up to a concentration of 75%. The precipitated protein was dissolved in buffer-A and subjected to gel filtration chromatography (Sephacryl-200), equilibrated with the same buffer on an AKTA BASIC FPLC system. Protein purity was checked by 12% SDS-PAGE (Supplementary data, Fig. S1) and all preparations used were at least 95% pure. Protein purity was also verified by electrospray ionization mass spectrometry (Supplementary data, Fig. S2A and B). Protein concentration was determined by Bradford's method (Bradford, 1976) using bovine serum albumin as a standard.

Enzyme activity

The enzyme activity of TIM was determined by the conversion of GAP to DHAP in the presence of TIM and α-glycerophosphate dehydrogenase (Oesper and Meyerhof, 1950; Plaut and Knowles, 1972). Enzymes were freshly prepared in 100 mM triethanolamine-HCl (TEA, pH 7.6). The reaction mixture contained (final volume 1 ml) 100 mM TEA, 5 mM EDTA, 0.5 mM NADH and α-glycerophosphate dehydrogenase (20 μg ml^{-1}), and 0.1–3 mM GAP. Enzyme activity was determined by monitoring the decrease in absorbance at 340 nm. The dependence of the initial rate on substrate concentration was analyzed according to the Michaelis–Menten equation. The values of the kinetic parameters (K_m, k_{cat}) were calculated from Lineweaver–Burk plots (Supplementary data, Fig. S3A and B). The data were analyzed by fitting to the Michaelis–Menten equation (1) as follows:

$$v = \frac{V_{max}[S]}{K_m + [S]} \quad (1)$$

where v and V_{max} are the initial velocity and maximum velocity, respectively, K_m is the Michaelis constant, and [S] is substrate concentration.

All initial rate data were first analyzed by double reciprocal plots of velocity versus substrate concentration and associated secondary plots. The data were then fitted by non-linear regression to standard kinetic models using Graph Pad Prism, version 4. The best-fit models were selected on the basis of goodness-of-fit (extra sum-of-squares F test) and P values. The kinetic parameters obtained by non-linear regression analysis were in agreement with the values obtained by Lineweaver–Burk plots and related secondary plots.

Size exclusion chromatography

Analytical gel filtration was performed on a Superdex-200 column (300 × 10 mm) attached to an AKTA BASIC FPLC system at a flow rate of 0.5 ml min^{-1}, and protein elution was monitored at a wavelength of 280 nm. The column was calibrated with β-amylase (200 kDa), alcohol dehydrogenase (150 kDa), bovine serum albumin (66 kDa), carbonic anhydrase (29 kDa) and cytochrome C (12.4 kDa).

Mass spectrometry

Electrospray ionization mass spectra were recorded on an Esquire 3000+ series mass spectrometer (Bruker Daltonics) coupled to an online 1100 series HPLC. Nebulization was assisted by N_2 gas (99.8%) at a flow rate of 10 l min^{-1}. The spray chamber was held at 250–300°C. The spectrometer

Downloaded from peds.oxfordjournals.org at Indian Institute of Science on May 26, 2011

was tuned to five calibration standards provided by the manufacturer. Data processing was done using the deconvolution module of the data analysis software to detect the multiple-charge states and obtain derived masses.

Fluorescence spectroscopy

Fluorescence emission spectra were recorded on a HITACHI-250 spectrofluorimeter. The protein samples were excited at 280 or 295 nm separately, and the emission spectra were recorded from 300 to 400 nm. Excitation and emission band passes were kept as 5 nm. Denaturation studies were done incubating 5 μM protein with different concentrations of urea and guanidium chloride (Gdmcl) for 45–60 min, and individual spectra were acquired from 300 to 450 nm after exciting the molecule at 295 nm.

Circular dichroism spectroscopy

Far UV–circular dichroism (CD) measurements were carried out on a JASCO-715 spectropolarimeter equipped with a thermostatted cell holder. The temperature of the sample solution in the cuvette was controlled with a Peltier device. For thermal melting studies, ellipticity changes at 222 nm were monitored to follow the unfolding transition. A cuvette of path length 1 mm was used and the spectra were averaged over four scans at a scanning speed of 10 nm min^{-1}. The change of ellipticity was measured as a function of temperature for thermal melting. Denaturation studies were done by incubating 5 μM of protein with different concentrations of urea and Gdmcl for 45–60 min and individual spectra (250–200 nm) were averaged out over three scans.

Structure visualization

All structural superpositions were carried out by secondary structure matching (Krissinel and Henrick, 2004) using COOT (Emsley and Cowtan, 2004). Hydrogen bonds and van der Waals contacts were identified using the CONTACT program of CCP4 suite based on distance criteria of 3.5 and 4.0 Å, respectively. The figures were generated using PyMol (DeLano, 2002).

Results

Kinetic parameters

The steady-state kinetics for WT and residue 13 mutants of PfTIM was measured by a coupled enzyme assay, using GAP as a substrate. The k_{cat}, K_m values for the wild-type enzyme C13D and C13E mutants are listed in Table I. The enzymes from the parasites *Trypanosoma brucei* and *Trypanosoma cruzi* also contain a cysteine residue at the structurally equivalent position (*T.brucei* C14, *T.cruzi* C15). Earlier studies by Hernández-Alcántara *et al*. (2002) and Zomosa-Signoret *et al*. (2007) have reported mutational studies at this position on the *T.brucei* TIM (TbTIM) and heterodimers of *T.brucei–T.cruzi* subunits harboring a C15A mutation. The kinetic data reported for these mutants are also listed in Table I for comparison. In these cases, Cys was replaced by neutral, polar and hydrophobic residues (Pérez-Montfort *et al*., 1999; Cabrera *et al*., 2008). Inspection of the data in Table I reveals that the C13D mutant shows an ~7.4-fold loss of activity, while the drop in k_{cat} is ~3.3-fold for the C13E mutant. In both the cases, there is no significant

Table I. Kinetic parameters of interface cysteine mutants from various sources[a]

Source	Mutants[b]	K_m (mM)	k_{cat} ($\times 10^5$) (min^{-1})	k_{cat}/K_m ($\times 10^5$) (mM^{-1} min^{-1})	T_m (°C)
P.falciparum[c]	WT	0.35 ± 0.16	2.68 ± 0.84	7.65	60.0
	C13D	0.31 ± 0.08	0.36 ± 0.07	1.16	43.8
	C13E	0.42 ± 0.05	0.82 ± 0.3	1.95	50.5
T.brucei[c,d]	WT	0.35 ± 0.05	2.6 ± 0.13	7.4	51.4
	C14A	0.43	3.1	7.2	50.3
	C14P	0.33	2.2	6.6	48.8
	C14S	0.5	3.0	6.0	48.8
	C14T	0.32	2.3	7.2	48.2
	C14V	0.42	2.4	5.7	47.9
	C14F	3.6 ± 1.3	0.012 ± 0.002	0.003	46.5
T.brucei[e]	WT	0.38 ± 0.04	2.5 ± 0.003	11.0	53.1
	C14S	0.5 ± 0.06	3.07 ± 0.01	10.3	47.9
	C14S/A69C	0.75 ± 0.04	1.56 ± 0.08	3.5	47.9
	C14S/S71C	0.35 ± 0.03	1.92 ± 0.06	9.1	47.1
	C14S/A73C	0.14 ± 0.03	2.89 ± 0.01	3.5	46.7
	C14S/S79C	4.8 ± 0.05	1.78 ± 0.08	6.2	44.7
T.cruzi[f]	TcTIM	0.45 ± 0.03	2.7 ± 0.02	6.0	–
T.brucei	TbTIM	0.46 ± 0.01	3.1 ± 0.05	6.7	–
	Interface mutant	0.4 ± 0.01	3.1 ± 0.03	7.7	–
	Tb:Tc TIM	0.31 ± 0.02	3.0 ± 0.02	9.6	–
	C15A TcTIM	0.42 ± 0.09	1.6 ± 0.02	3.8	–
	C15A Tc–Tb TIM	0.28 ± 0.09	1.3 ± 0.02	4.6	–
	C15A Tc–Tb MMTS	0.62 ± 0.09	0.5 ± 0.02	0.8	–

[a]The values listed are for enzyme assays done using GAP as a substrate (described in Materials and methods section).
[b]The residue numbering schemes for PfTIM, TbTIM and TcTIM are different. C13 of *P.falciparum* is structurally equivalent to C14 of *T.brucei* and C15 of *T.cruzi*.
[c]This study.
[d]Hernández-Alcántara *et al*. (2002).
[e]Zomosa-Signoret *et al*. (2007).
[f]Cabrera *et al*. (2008)

Downloaded from peds.oxfordjournals.org at Indian Institute of Science on May 26, 2011

change in K_m, as compared with WT enzyme. Previously published data for the TbTIM suggest that replacement of Cys14 with Ala, Pro, Ser, Thr and Val has little effect on enzymatic activity. In contrast, the C14F mutant shows a significant reduction (~216-fold) in k_{cat} and a 10-fold increase in K_m (Cabrera *et al*., 2008). These results establish that substrate binding is not appreciably affected in the C13D and C13E mutants of PfTIM, while k_{cat} shows a significant reduction.

The concentration dependence of enzyme activity was also measured for the C13E mutant over the range 0.2–1.2 μM. There was no dependence of specific activity.

Analytical gel filtration

Figure 3 shows the analytical gel filtration profile of TIM WT and the Cys13 mutants at two different protein concentrations. At a protein concentration of 2.5 μM, the WT enzyme and the Cys13 mutants show a single peak at ~13.9 ml, which confirms the dimeric structure of the protein. Thus at this protein concentration, the mutations have no effect on the overall tertiary structure of the enzyme. The next set of analytical gel filtration experiments was performed at 1.25 μM protein concentration for WT as well as the Cys13 mutants. Interestingly, the WT and the C13E mutant elute as a single peak at ~13.9 ml, suggesting that at this concentration both the enzymes retain their dimeric structure. In sharp contrast, the C13D mutant shows two distinct peaks at ~13.9 and ~15.5 ml. This observation suggests that the C13D mutation appears to destabilize the dimer interface, resulting in subunit dissociation. In an earlier report from this laboratory, a sharp fall in measured enzymatic activity was observed in the concentration range 0.2–0.6 μM for the C13D mutant (Maithal *et al*., 2002).

Effect of chemical denaturants

The $(\beta/\alpha)_8$ barrel structure in PfTIM retains considerable secondary and tertiary structure even in the presence of 8 M urea. However, the protein has been shown to unfold readily in the presence of Gdmcl) solutions, at a denaturant concentration of ~2.5 M (Gokhale *et al*., 1999). Unfolding may be conveniently monitored by measuring the fluorescence emission spectrum, which arises from contributions due to Trp11 and Trp168 (Pattanaik *et al*., 2003). Figure 4A and C compares the change in fluorescence emission maxima (λ_{max}) as a function of urea and Gdmcl concentration for WT PfTIM (TWT), C13D and C13E mutants. The emission maximum of WT and the C13D mutant is 331 nm, while λ_{max} for the C13E mutant is 333 nm. Upon addition of urea, all three proteins showed a shift of the emission maximum to longer wavelength, suggesting enhanced solvent exposure of the side chain of Trp residues. In the case of TIM WT, this red shift of emission is observed only at urea concentrations >5 M. In sharp contrast, the change in fluorescence properties occurs at a significantly lower concentration (2–4 M) of urea in the case of C13D and C13E mutants. Evidently, weakening of subunit interface interactions contributes appreciably to the Cm (midpoint of the transition curve) of the urea denaturation process. Interestingly, in the case of Gdmcl the distinction between the three proteins is less dramatic, although the midpoint of the unfolding transition follows the order TWT > C13E > C13D. Figure 4B and D summarizes the unfolding profiles obtained with the three proteins in urea and Gdmcl solutions using CD ellipticity at 222 nm (θ_{222}) as a probe. It is

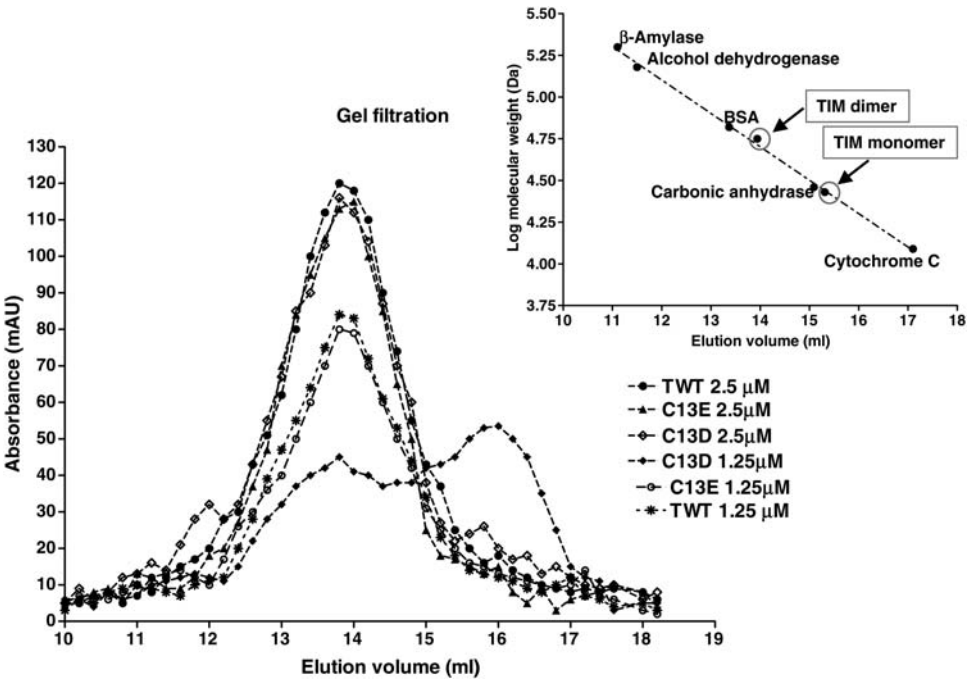

Fig. 3. Analytical gel filtration profile for PfTIM wild type (WT) and C13D and C13E mutants at two different concentrations. The column used for gel filtration was 10 mm × 30 cm long containing Superdex-200 (S-200) resin. The buffer containing 25 mM Tris–HCl (pH 8.0) with 100 mM sodium chloride was used for all the runs at a flow rate of 0.5 ml min^{-1}. At both 2.5 and 1.25 μM TIM WT and C13E mutant eluted as a single peak at ~13.9 ml. However, the C13D mutant showed two peaks at ~13.9.0 and ~15.5 ml. The relative retention volumes of molecular weight markers are shown in the inset.

Downloaded from peds.oxfordjournals.org at Indian Institute of Science on May 26, 2011

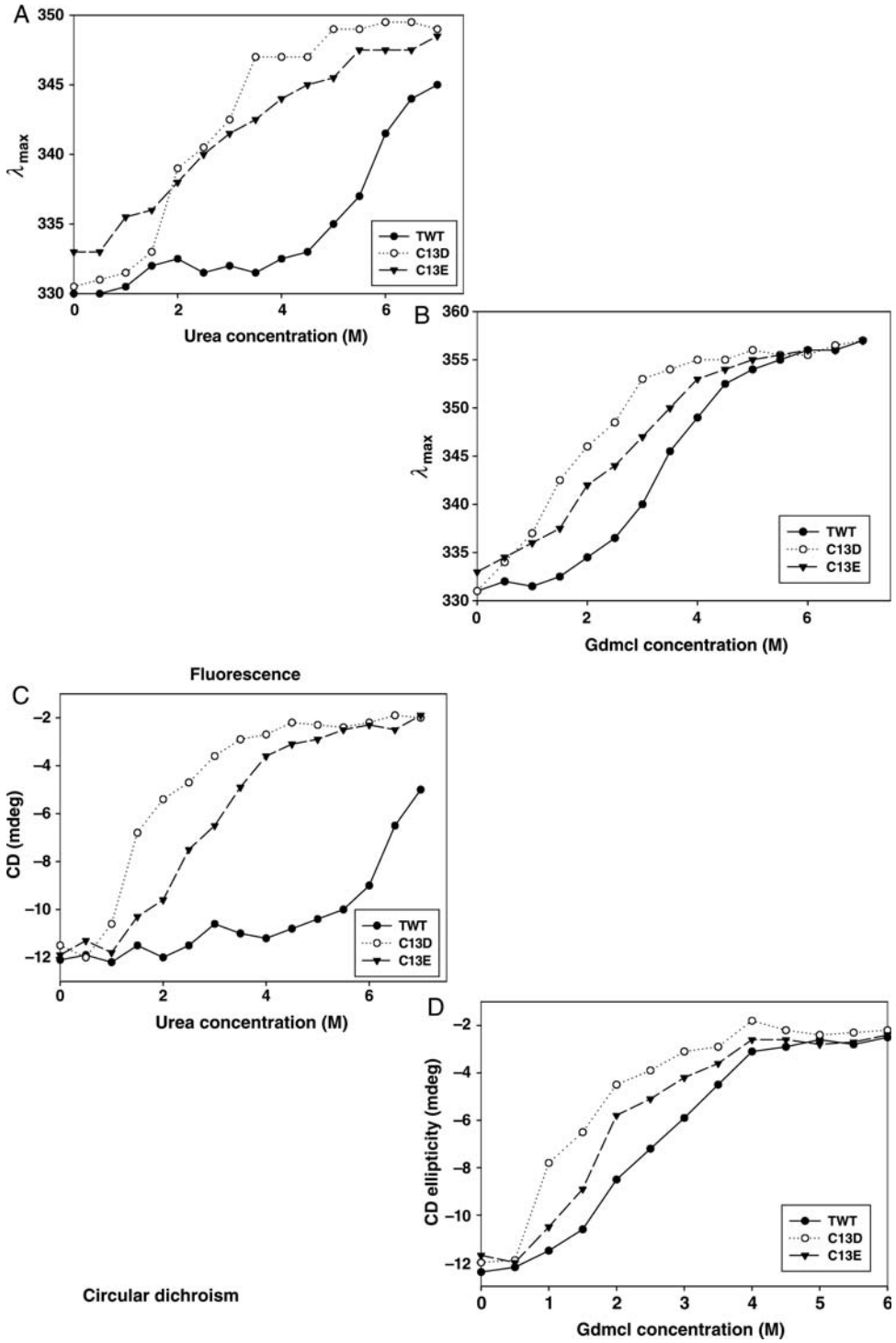

Fig. 4. Equilibrium unfolding of PfTIM WT and mutants was studied in the presence of the denaturing agents, urea and Gdmcl. Unfolding profiles were observed after incubating the respective proteins at different concentrations of urea and Gdmcl for 1 h. Unfolding was monitored by fluorescence and CD. (**A**) Change in emission maxima is plotted against urea concentration. (**B**) Change in ellipticity (θ) at 222 nm (θ in mdeg) is plotted against urea concentration. Similarly, (**C**) change in emission maxima is plotted against Gdmcl concentration. (**D**) Change in ellipticity (θ) at 222 nm (θ in mdeg) is plotted against Gdmcl concentration. The experiments were carried out in 20 mM Tris–HCl (pH 8.0).

clearly seen that the order of stability in urea solution is TWT > C13E > C13D, and a similar conclusion may be drawn from the Gdmcl data (Fig. 4D).

Thermal denaturation

PfTIM WT undergoes irreversible thermal precipitation at ~60°C, a process attributed to the formation of protein aggregates through unfolding intermediates (Gopal *et al*., 1999). This process can be conveniently monitored by observing the drop in CD ellipticity at 222 nm (θ_{222}) or the increase in Rayleigh scattering upon aggregation. Figure 5 compares the changes in ellipticity for PfTIM WT and the mutants C13D and C13E. It is clearly evident that the mutants undergo thermal denaturation at much lower temperatures, with the

Downloaded from peds.oxfordjournals.org at Indian Institute of Science on May 26, 2011

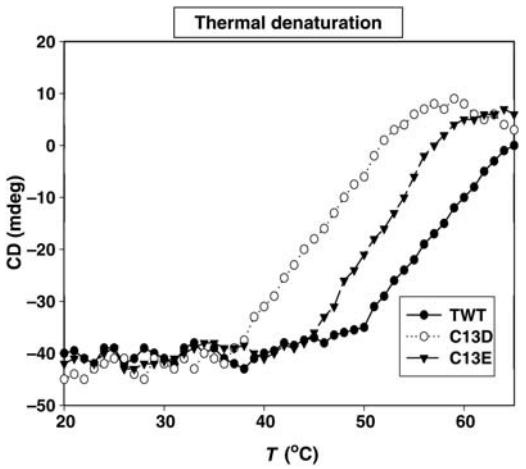

Fig. 5. Temperature-dependent denaturation curves for cysteine mutants (C13D and C13E) along with TIM WT measured using CD. The data have been generated by monitoring the CD ellipticity at a wavelength of 222 nm at a rate of increasing temperature of $1^{\circ}C\ min^{-1}$ from 20 to 65°C. Irreversible thermal precipitation is observed during the course of study. Ten micromolar protein (0.4 mg ml^{-1}) in 5 mM Tris–HCl at pH 8.0 was used in each case.

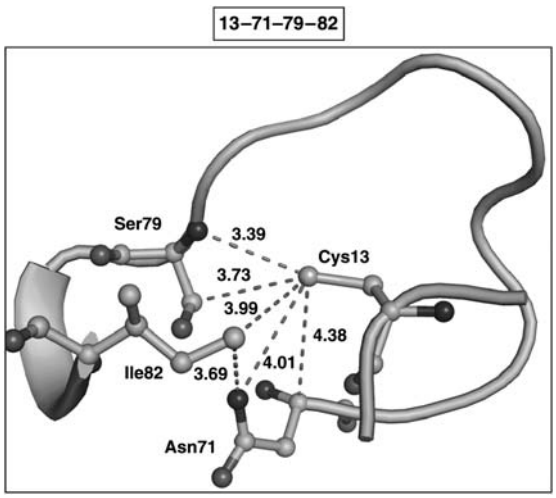

Fig. 6. The crucial contacts of residue 13 of subunit A with residues 71, 79 and 82 of subunit B are shown here. The C^{α} traces of loop 1 (partial) and loop 3 are shown in ribbon diagram. The contacts of Cys 13 thiol SH with side chain NH of Asn71, backbone CO of Ser79 and side chain C^{δ} methyl group of Ile82 are marked. The 3D coordinates have been taken from PfTIM structure (PDB ID 1O5X) and the figure has been generated in PyMol (DeLano, 2002).

C13D mutant being the most fragile. The measured melting temperatures (T_m, °C) are listed in Table I, which also provides comparative data obtained previously for trypanosomal TIMs (Hernández-Alcántara *et al*., 2002). The C13D mutant is appreciably less stable than the C13E mutant, consistent with the results obtained for chemical denaturation. Indeed, the C13D mutant has the lowest T_m value, 43.8°C, of all the mutants listed in Table I.

Discussion

The kinetic and spectroscopic data presented above established that the introduction of a negatively charged residue at position 13 in PfTIM results in catalytically impaired mutants, which also display a significantly lower degree of structural stability. The analytical gel filtration further suggests that the C13D mutant shows a significantly enhanced tendency to dissociate into monomers. The vast body of structural data on TIM from different sources has established that dimerization is indeed critical for maintenance of enzymatic activity. Attempts to monomerize TIM have resulted in the engineering of structurally stable mono-TIMs (Borchert *et al*., 1993, 1994), which, however, have catalytic activities that are reduced by a factor of 1000 when compared with the native enzyme. As seen from Fig. 1, two residues Thr75 and Cys13 are involved in the largest number of close inter-subunit contacts, presumably contributing to the stability of the dimer interface. Inspection of the crystal structure reveals that the completely conserved Thr75 residues make crucial hydrogen bonding contacts with the other subunit, which appear to be essential for holding the active site residues in an appropriate geometry (Banerjee *et al*., 2009). Figure 2 shows a view of residue C13 and the close contacts that it makes with loop 3 residues (69–79) from the neighboring subunit. The availability of a large number of TIM sequences from diverse organisms prompted us to examine the nature of residues occurring at this position and proximal interacting sites on the proteins. Figure 2B summarizes a survey of 470 (eukaryotic and bacteria) TIM sequences, which reveals that position 13 is largely occupied by apolar amino acid residues such as Met and Leu, with very few examples of polar residues. Significantly, there are no reported occurrences of positively charged residues at this position. The sulfur atom of Cys13 appears to be close packed with Ser79 and Ile82 side chains as seen in Fig. 6. In order to examine the steric perturbation caused by the C13D and C13E mutations, we modeled the side chains at position 13 and examined contacts made for various rotameric states, chosen from a library (Fig. 7). Interestingly, the carboxylate of Asp13 is positioned to make a reasonably good hydrogen bond contact with the backbone NH group of Ser79. However, short contacts are observed with the C^{δ} methyl group of Ile82. In contrast, the more extended Glu13 side chain can be accommodated at this position without this unfavorable contact. An unacceptably short hydrogen bond distance to Ser79 may be relieved by minor conformational adjustments. The modeling result suggests that the C13D mutation is anticipated to result in greater structural perturbation than the C13E mutation. This is, indeed, consistent with the experimental results where a significantly greater drop in k_{cat} (~7.4-fold) is observed for the C13D mutant, while the fall in activity is lower for the C13E mutant (~3.3-fold). The greater tendency of the C13D mutant to dissociate lends further support to the conclusion that introduction of the smaller aspartyl side chain results in a greater perturbation than the larger glutamyl side chain at this position.

The C13D andC13E mutants of PfTIM show a significant reduction in k_{cat}. A question that needs to be addressed is whether the fall in activity observed for the C13D and C13E mutants is due to a reduction in the number of catalytically competent dimers present at the concentrations used in the enzyme assay, or whether a structural perturbation in the vicinity of the active site results in the attenuation of enzyme activity. The concentration dependence of specific activity of the C13D mutant has been previously reported (Maithal

Downloaded from peds.oxfordjournals.org at Indian Institute of Science on May 26, 2011

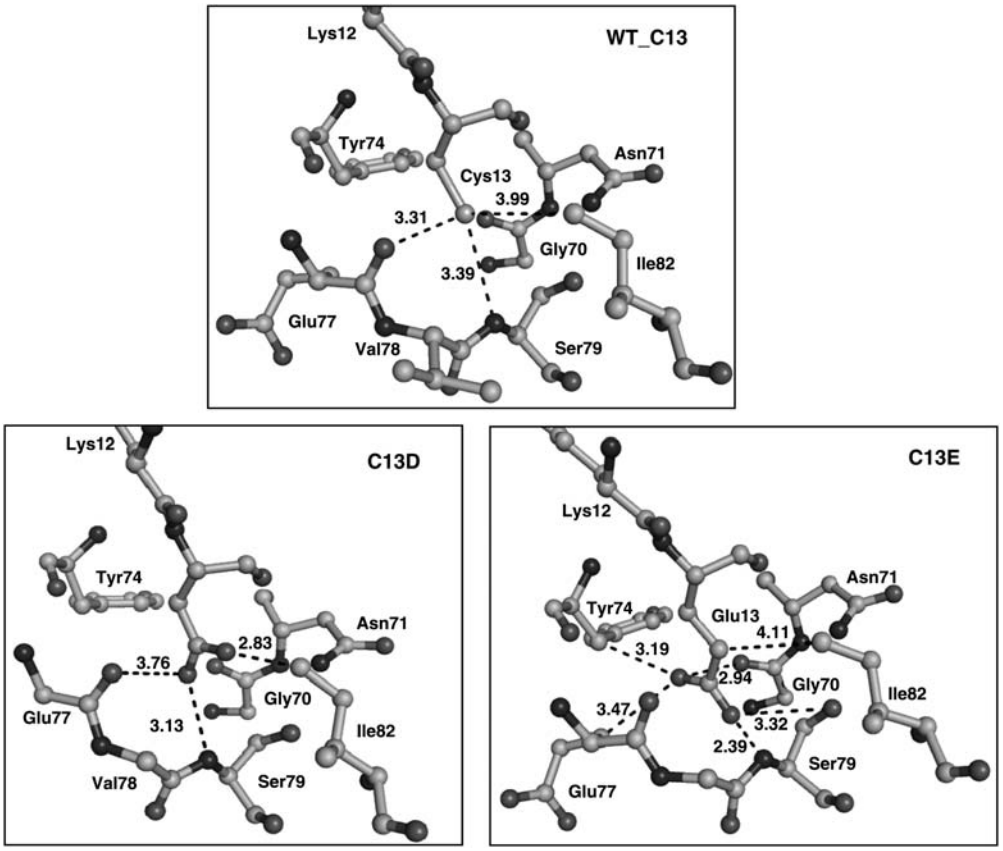

Fig. 7. The environments of C13, C13D and C13E mutants (modeled) in PfTIM are shown as ball and stick. (A) The image has been generated using the coordinates of PfTIM (PDB ID 1O5X). (B and C) The side chains of C13D and C13E mutants have been modeled on the WT template to examine the different rotameric contact mates. The best rotamer among the library has been chosen to compare the C13D and C13E mutants.

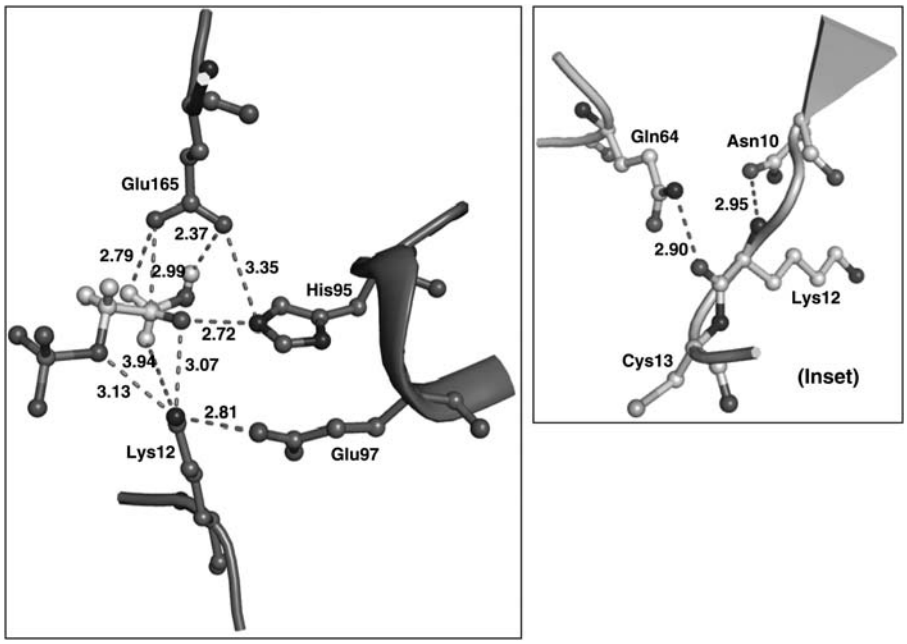

Fig. 8. Active site residues of yeast TIM–DHAP complex (Jogl *et al.*, 2003) and their orientation upon substrate/ligand binding are shown as ball and stick. Inset shows the unusual backbone conformation of Lys12 residue and the crucial hydrogen bonds with Asn10 and Gln64.

et al., 2002). Above a threshold of 0.6 μM, there was no concentration dependence of activity, suggesting that catalytic dimers were indeed present under these conditions. In the case of C13E, the mutant dimers were indeed more robust and there was no concentration dependence of specific activity even in the range from 0.2 to 0.6 μM. It therefore appears reasonable to examine the possible structural effects of mutations at residue 13 on the active site, in view of the

Downloaded from peds.oxfordjournals.org at Indian Institute of Science on May 26, 2011

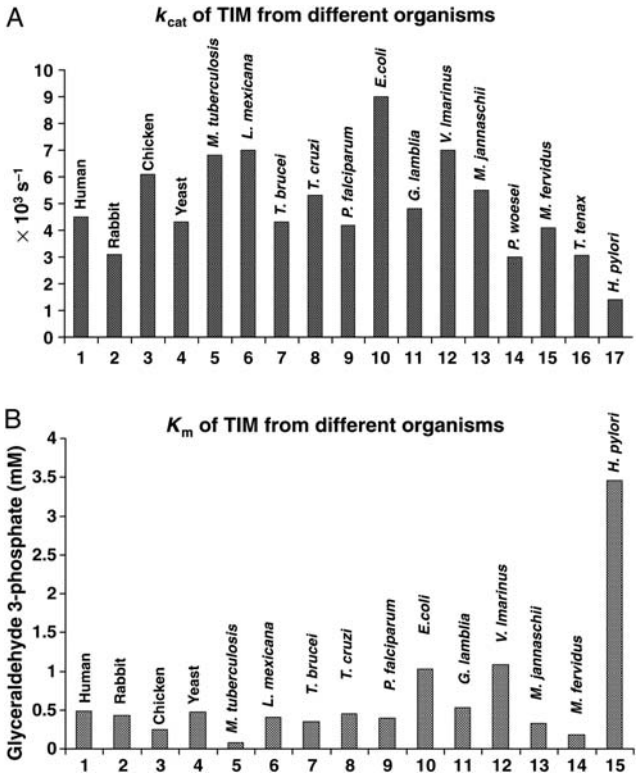

Fig. 9. Comparison of the kinetic parameters of TIM from different sources. (**A**) The k_{cat} values (min^{-1}) and (**B**) the K_m (mM) values (GAP as a substrate) are plotted.

proximity of the site of mutation to the active site Lys12 residue.

The precise positioning of the Lys ε-NH_3+ with respect to the substrate is undoubtedly necessary for optimal catalysis. Figure 8 shows a view of the conserved residues of TIM oriented about the substrate DHAP (Jogl *et al*., 2003). The Lys12 residue is critical for activity and is held in place by Asn10 and Gln64, both of which are almost completely conserved in all TIM sequences. Indeed in the 470 (bacterial, eukaryotic) dataset, position 64 is occupied by Gln in 442 and Glu in 28, whereas residue 10 has Asn in 465 and Ser in 5 sequences. The Glu–Gln and Asn–Ser replacements will leave the hydrogen bonds to the Lys backbone unaffected. This feature appears to be critical in maintaining TIM activity, since the Lys12 residue adopts unusual Ramachandran ϕ, ψ values ($\phi = 54.3 \pm 5.5$, $\psi = -144.1 \pm 7.0$) in all 24 crystal structures from different organisms determined thus far (Banerjee *et al*., 2009). Residue 13, the site of mutation in the present study, is adjacent in sequence to this critical residue as seen in Fig. 8.

Inspection of Fig. 6 suggests that the inter-residue interaction across the subunit interface may make an important contribution to dimer stability and enzymatic activity. Residue 13(A) makes crucial contacts with the backbone CO of residue 79 (B), the backbone NH of residue 71(B) and the side chain of residue 82(B). Investigation of natural TIM sequences provides the distribution of amino acids at positions 13 and 82 as a coevolving pair. Using the 470 sequence dataset, the following 13(A)/82(B) doublets are observed: M/M 259, L/M 54, M/Q 33, N/A 33, C/M 14, M/V 13 and M/F 11. These account for 374 examples of the total dataset. However, both the positions do not contain a charged residue. In spite of the large amino acid diversity at positions 13 and 82, the absence of charged residues in natural sequences is suggestive of a selective pressure in the selection of amino acids at these positions in order to maintain the enzyme fold and function.

In the natural sequences, accommodation of a Cys residue at position 13 (22 examples) results in only Met (14), Ile (4), His (3) and Gln (1) at the corresponding position 82. Crystal structures are available for the C13/M82 pair (three examples) and the C13/I82 pair (four examples). These four examples of the C13 (A)/I82 (B) doublet are in the enzymes from *P.falciparum*, *T.brucei*, *T.cruzi* and *Leishmania mexicana.* Interestingly, crystal structures are available in all the cases. The three examples of the doublet Q13/Q82 are of special interest since the side chain would resemble the Glu side chain introduced in the present study, at this position. In all three cases, residue 13 from subunit A and residue 82 from subunit B (13A/82B) pairs are from three different organisms, *Moraxella*, *Psychrobacter arcticus* and *Psychrobacter cryohalolentis*. In spite of the apparent diversity of residues at this position, it is clear that only a limited number of pairs are in fact compatible for the requirements of subunit assembly and enzyme activity. Structural analyses of these TIMs or of the engineered double mutants should provide further insights.

Despite the complete exclusion of charged amino acids at position 13 in natural TIM sequences, the engineered C13E mutant is only ~3-fold less active than the WT enzyme. Figure 9 provides a comparison of the k_{cat} value reported for TIMs from diverse organisms. However, reservation might be expressed about the advisability of comparing k_{cat} values determined for enzymes from different organisms from different groups of investigators sometimes using distinct protocols. It is notable that for TIM all the determined k_{cat} values fall within a relatively limited range; k_{cat} mean including *Helicobactor pylori* is $(3.33 \pm 1.0) \times 10^5\ min^{-1}$ and excluding *H.pylori* is $(3.14 \pm 1.17) \times 10^5$. The lowest reported value thus far is for *H.pylori*, which also has the highest reported value of K_m (~3.46 ± 0.23 mM) (Chu *et al*., 2007). The measured activity for the C13E mutant is clearly below the threshold for all naturally occurring TIMs studied at the present time, suggesting that impaired catalytic activity may be selected out if it significantly affects the flux of glycolysis in an organism. Mutational analysis guided by comparisons between the growing numbers of natural sequences may be valuable in identifying coevolving segments of proteins (Halabi *et al*., 2009), which are important for the maintenance of structure and function.

Supplementary data

Supplementary data are available at *PEDS* online.

Acknowledgements

M.B. thanks the Council for Scientific and Industrial Research, Government of India, for award of a Senior Research Fellowship.

Funding

The mass spectral facility was supported under the Proteomics program of the Department of Biotechnology (DBT). This research was supported by a program grant from

Downloaded from peds.oxfordjournals.org at Indian Institute of Science on May 26, 2011

the DBT and a grant from the Department of Science and Technology (DST).

References

Albery,W.J. and Knowles,J.R. (1976a) *Biochemistry*, **15**, 5631–5640.

Albery,W.J. and Knowles,J.R. (1976b) *Biochemistry*, **15**, 5627–5631.

Banerjee,M., Balaram,H. and Balaram,P. (2009) *FEBS J.*, **276**, 4169–4183.

Borchert,T.V., Abagyan,R., Kishan,K.V., Zeelen,J.P. and Wierenga,R.K. (1993) *Structure*, **1**, 205–213.

Borchert,T.V., Abagyan,R., Jaenicke,R. and Wierenga,R.K. (1994) *Proc. Natl. Acad. Sci. USA*, **91**, 1515–1518.

Bradford,M.M. (1976) *Anal. Biochem.*, **72**, 248–254.

Cabrera,N., Hernández-Alcántara,G., Mendoza-Hernández,G., Gómez-Puyou,A. and Perez-Montfort,R. (2008) *Biochemistry*, **47**, 3499–3506.

Casal,J.I., Ahern,T.J., Davenport,R.C., Petsko,G.A. and Klibanov,A.M. (1987) *Biochemistry*, **26**, 1258–1264.

Chu,C.H., Lai,Y.J., Huang,H. and Sun,Y.J. (2007). *Proteins Struct. Funct. Bioinform.*, **71**, 396–406.

Cortés-Figueroa,A.A., Pérez-Torres,A., Salaiza,N., Cabrera,N., Escalona-Montaño,A., Rondán,A., Aguirre-García,M., Gómez-Puyou,A., Pérez-Montfort,R. and Becker,I. (2008) *Parasitol. Res.*, **102**, 635–643.

Cui,Q. and Karplus,M. (2003) *Adv. Protein Chem.*, **66**, 315–372.

DeLano,W.L. (2002) *The PyMOL Molecular Graphics System*. DeLano Scientific, San Carlos, CA.

Dwyer,M.A., Looger,L.L. and Hellinga,H.W. (2004) *Science*, **304**, 1967–1971; Rétraction.

Dwyer,M.A., Looger,L.L. and Hellinga,H.W. (2008) *Science*, **319**, 569b.

Emsley,P. and Cowtan,K. (2004) *Acta Crystallogr. D Biol. Crystallogr.*, **60**, 2126–2132.

Garza-Ramos,G., Pérez-Montfort,R., Rojo-Domínguez,A., de Gómez-Puyou,M.T. and Gómez-Puyou,A. (1996) *Eur. J. Biochem.*, **241**, 114–120.

Gayathri,P., Banerjee,M., Vijayalakshmi,A., Azeez,S., Balaram,H., Balaram,P. and Murthy,M.R.N. (2007) *Acta Crystallogr. D Biol. Crystallogr.*, **63**, 206–220.

Gokhale,R.S., Ray,S.S., Balaram,H. and Balaram,P. (1999) *Biochemistry*, **38**, 423–431.

Gómez-Puyou,A., Saavedra-Lira,E., Becker,I., Zubillaga,R.A., Rojo-Domínguez,A. and Pérez-Montfort,R. (1995) *Chem. Biol.*, **2**, 847–855.

Gopal,B., Ray,S.S., Gokhale,R.S., Balaram,H., Murthy,M.R.N. and Balaram,P. (1999) *Biochemistry*, **38**, 478–486.

Halabi,N., Rivoire,O., Leibler,S. and Ranganathan,R. (2009) *Cell*, **138**, 774–786.

Hernández-Alcántara,G., Garza-Ramos,G., Mendoza-Hernández,G., Gómez-Puyou,A. and Pérez-Montfort,R. (2002) *Biochemistry*, **41**, 4230–4238.

Jogl,G., Rozovsky,S., McDermott,A.E. and Tong,L. (2003) *Proc. Natl. Acad. Sci. USA*, **100**, 50–55.

Joubert,F., Neitz,A.W.H. and Louw,A.I. (2001) *Proteins Struct. Funct. Genet.*, **45**, 136–143.

Knowles,J.R. (1991) *Nature*, **350**, 121–124.

Krissinel,E. and Henrick,K. (2004) *Acta Crystallogr. D Biol. Crystallogr.*, **60**, 2256–2268.

Lodi,P.J. and Knowles,J.R. (1991) *Biochemistry*, **30**, 6948–6956.

Maithal,K., Ravindra,G., Balaram,H. and Balaram,P. (2002) *J. Biol. Chem.*, **277**, 25106–25114.

Oesper,P. and Meyerhof,O. (1950). *Arch. Biochem.*, **27**, 223–233.

Ostoa-Saloma,P., Garza-Ramos,G., Ramirez,J., Becker,I., Berzunza,M., Landa,A., Gomez-Puyou,A., Tuena de Gomez-Puyou,M. and Perez-Montfort,R. (1997) *Eur. J. Biochem.*, **244**, 700–705.

Pattanaik,P., Ravindra,G., Sengupta,C., Maithal,K., Balaram,P. and Balaram,H. (2003) *Eur. J. Biochem.*, **270**, 745–756.

Pérez-Montfort,R., Garza-Ramos,G., Hernández Alcántara,G., Reyes-Vivas,H., Xiu-gong,G., Maldonado,E., Tuena de,M. and Gómez-Puyou,A. (1999) *Biochemistry*, **38**, 4114–4120.

Plaut,B. and Knowles,J.R. (1972) *Biochem. J.*, **129**, 311–320.

Putman,S.J., Coulson,A.F., Farley,I.R., Riddleston,B. and Knowles,J.R. (1972) *Biochem. J.*, **129**, 301–310.

Ranie,J., Kumar,V.P. and Balaram,H. (1993) *Mol. Biochem. Parasitol.*, **61**, 159–169.

Rieder,S.V. and Rose,I.A. (1959) *J. Biol. Chem.*, **234**, 1007–1010.

Sambrook,J. and Russell,D.W. (2001) *Molecular Cloning: A Laboratory Manual*, 3rd edn. Cold Spring Harbor Laboratory Press, Cold Spring Harbor, NY.

Sarkar,G. and Sommer,S.S. (1990) *BioTechniques.*, **8**, 404–407.

Schliebs,W., Thanki,N., Jaenicke,R. and Wierenga,R.K. (1997) *Biochemistry*, **36**, 9655–9662.

Singh,S.K., Maithal,K., Balaram,H. and Balaram,P. (2001). *FEBS Lett.*, **501**, 19–23.

Walden,H., Bell,G.S., Russell,R.J., Siebers,B., Hensel,R. and Taylor,G.L. (2001) *J. Mol. Biol.*, **306**, 745–757.

Webb,M.R. and Knowles,J.R. (1974) *Biochem J.*, **141**, 589–592.

Webb,M.R. and Knowles,J.R. (1975) *Biochemistry*, **14**, 4692–4698.

Wierenga,R.K., Kalk,K.H. and Hol,W.G. (1987) *J. Mol. Biol.*, **198**, 109–121.

Wierenga,R.K., Kapetaniou,E.G. and Venkatesan,R. (2010) *Cell. Mol. Life Sci.*, **67**, 3961–3982.

Zomosa-Signoret,V., Aguirre-López,B., Hernández-Alcántara,G., Pérez-Montfort,R., Tuena de,M., Gómez-Puyou,. and Gómez-Puyou,A. (2007) *Proteins Struct. Funct. Bioinform.*, **67**, 75–83.

View publication stats

Downloaded from peds.oxfordjournals.org at Indian Institute of Science on May 26, 2011